batteries

MDPI

*Review*

# Review of Lithium-Ion Battery Internal Changes Due to Mechanical Loading

**Maria Cortada-Torbellino, David Garcia Elvira, Abdelali El Aroudi * and Hugo Valderrama-Blavi**

Department of Electronics, Electrical Engineering and Automatic Control, Universitat Rovira i Virgili, 43007 Tarragona, Spain

* Correspondence: abdelali.elaroudi@urv.cat

**Abstract:** The growth of electric vehicles (EVs) has prompted the need to enhance the technology of lithium-ion batteries (LIBs) in order to improve their response when subjected to external factors that can alter their performance, thereby affecting their safety and efficiency. Mechanical abuse has been considered one of the major sources of LIB failure due to the changes it provokes in the structural integrity of cells. Therefore, this article aims to review the main factors that aggravate the effects of mechanical loading based on the results of different laboratory tests that subjected LIBs to abusive testing. The results of different cell types tested under different mechanical loadings have been gathered in order to assess the changes in LIB properties and the main mechanisms responsible for their failure and permanent damage. The main consequences of mechanical abuse are the increase in LIB degradation and the formation of events such as internal short circuits (ISCs) and thermal runways (TRs). Then, a set of standards and regulations that evaluate the LIB under mechanical abuse conditions are also reviewed.

**Keywords:** lithium-ion batteries (LIBs); electric vehicle (EV); mechanical abuse; LIB degradation; regulations; internal short circuit (ISC)



**Citation:** Cortada-Torbellino, M.; Elvira, D.G.; El Aroudi, A.; Valderrama-Blavi, H. Review of Lithium-Ion Battery Internal Changes Due to Mechanical Loading. *Batteries* **2024**, *10*, 258. https://doi.org/10.3390/batteries10070258

Academic Editor: Carlos Ziebert

Received: 6 May 2024
Revised: 28 June 2024
Accepted: 3 July 2024
Published: 22 July 2024



## 1. Introduction

The global awareness regarding climate change and carbon footprints has led the vehicle industry to invest its resources in the development of lower-emission vehicles. Over the years, the predominant technology has been the electric vehicle (EV), which is mainly powered by lithium-ion batteries (LIBs). Despite the impressive results achieved by LIBs regarding energy density and manufacturing costs, certain aspects pertaining to safety still require further improvements.

One of the major concerns regarding LIBs is their capability to develop an internal short circuit (ISC) due to changes in their internal properties after being subjected to numerous charge/discharge cycles, vibrations, high temperatures, or a vehicle collision. The development of an ISC can also initiate a thermal runway (TR). A TR is characterized by an uncontrollable temperature rise triggered by an exothermic process that results in the failure of the LIB or, under extreme circumstances, a fire in the system [1].

Therefore, in order to develop a TR, the LIB must suffer from an ISC, which will increase the temperature of certain areas due to the electric heat generated. This will also cause an increment in the temperature of surrounding spots, causing a temperature rise in the entire cell [2,3].

The temperature increase from the TR process can be divided into three different stages. During the first stage, the LIB operates under a safe temperature range. In the second stage, the temperature rise initiates separator melting, and irreparable damage begins. Finally, during the third stage, complete LIB failure occurs [4–8].

The consequences of the TR depend on different factors, such as the SOC, which has been investigated in [9] through the comparison of the thermal stability of different LIB

chemistries (NCA/graphite, LFP/graphite, and NCA/LTO), charged at different SOC levels (0%, 50%, and 100%). The authors observed a significant heating increase for cells loaded at higher SOC. Results from [10] reached the same conclusion after assessing the thermal stability of three different cylinder cells (18650, 20700, and 26650) and two different chemistries (LFP/graphite and NCA/graphite).

A further influencing factor behind the consequences of TR that has been reported in [11] is the cell capacity. This article aimed to assess the self-heating stages of pouch cells with a capacity range of 33–3300 mAh. The sudden voltage drop observed was associated with the exothermic reactions that resulted from the consumption of the cathode and separator after the temperature increase [12]. This phenomenon was not observed in cells with lower capacities (33 mAh) but was predominant in cells with higher capacities (1000–3300 mAh), which also experienced a higher temperature increase [11].

A TR has been recently reported in a Tesla Model S, which caught fire due to the heat generated in the LIB [13]. The accident can be seen in Figure 1.


**Figure 1.** Tesla Model S on a fire accident due to the heat generated in the LIB.

Different abuse methods have been found to damage the LIB and induce TR. These methods can be categorized into thermal, electrical, and mechanical abuse [14]. Thermal abuse can originate from overheating conditions and fire exposure. Overcharge/over-discharge and ISC are considered to be electrically abusive conditions due to the abnormal operation of electrical components [15]. Physical cell deformation and displacement are established as mechanical abuse conditions [16,17].

The safety of EVs has become one of the major public concerns as they exhibit distinct kinematic characteristics in comparison to internal combustion engine vehicles (ICEs), owing to their distinct acceleration performance and mechanical structure. This indicates potentially distinct safety behaviors. For instance, the mass of the LIB can increase the global vehicle weight by 450 kg to 900 kg; therefore, EVs need to dissipate more kinetic energy when involved in a collision compared to an ICE vehicle [18]. Furthermore, the risk of being involved in a road accident is not only associated with injuries to occupants and pedestrians due to the crash itself but also due to battery incidents [19]. Possible exposure to a vehicle collision is one of the main sources of mechanical abuse due to the deformation and fracture of different cell components that could lead to the formation of an ISC or TR [20,21].

The presence of ISC and TR after mechanically abusive scenarios has been investigated in different studies, such as [22], which aimed to evaluate the response of LIBs under quasi-static mechanical loading using four test protocols: circular punch, rod, flat plate, and three-point bend. The results indicated cell failure, as a sudden force drop was observed

during the initiation of the ISC. Another mechanical abusive test is nail penetration, which was employed in [23] to evaluate the TR development. The article concluded that the origin of the heat that leads to a TR comes from the dissolution of the separator and the heat from the ISC. Moreover, considering that cylinder cells are the most common type of cell in EVs, authors from [24] submitted them to a lateral crash in order to assess their defamation and address the risk of ISC under extreme mechanical loading. Furthermore, the cell response under mechanical abuse can be affected by the SOC since cells charged at higher SOC suffer from larger stress conditions and thus can suffer from an ISC under smaller displacement. Therefore, cells loaded at higher SOC can be more dangerous during a crash from the mechanical perspective [25].

Even though one of the main consequences of a vehicle impact is global cell compression and the formation of cracks on the separator, welding breakage, and vibrations from transportation and daily movement have been demonstrated to be another source of mechanical failure due to the durability affectations of the LIB components. The aim of vibration testing is to replicate the road vibration profile in order to identify any potential damage that could occur to the device, such as welding breakage [26].

Since providing a safe performance is of significant importance, different tests and safety standards have emerged as a highly advantageous method to comprehend their behavior under mechanical loading, such as SAEJ2464, UL1973, GB/T36276, and IEC62660-2 [27]. However, even though the safety assessment of LIBs comprises various tests that must be successfully completed, there are instances where they exhibit a lack of resemblance to real EVs. For instance, cells from LIBs are located in the battery module, which generates a different force distribution in contrast to single-cell testing. Therefore, feasible and consistent tests must be performed in order to obtain accurate results [28,29]. A brief overview of the main current methods employed to anticipate hazardous events at the testing level on EVs is provided in this study.

LIB properties can change when exposed to mechanical loads originating from an abusive scenario, such as vehicle collisions or the impact of road objects [20,30,31]. Moreover, mechanical loading can also produce internal cell damage, such as electrode and separator fracture, which are one of the main causes of TR, as long as there is ISC formation [32,33]. Then, considering that the hazard level of mechanical abuse depends on different factors, this article aims to review the effects that the compression, impact direction, presence of electrolytes, SOC level, and aging have on the LIB response when submitted to mechanical damage.

This paper is organized as follows. After the previous introduction, Section 2 provides an overview of the testing methods, while the response of mechanical loading on LIB integrity is described in Section 3. Finally, conclusions are drawn in Section 4.

## 2. Safety Standards and Regulations for Mechanical Abuse Assessment

Given the increasing demand for LIBs in the market, the need to develop a series of standards and regulations to ensure their safety has increased. Different testing procedures have been developed to address safety requirements, with the aim of enhancing the design of the LIB, improving their weak points and protection systems, and offering guidance toward comprehending failure mechanisms.

The assessment procedures of LIBs can be distinguished between standards and regulations. On the one hand, standard tests are non-mandatory procedures developed by different organizations at the international level, such as the International Electrotechnical Commission (IEC), the International Organization for Standardization (ISO), the Society of Automotive Engineers (SAE), the Institute for Electrical and Electronics Engineering (IEEE), and the Infrastructure Working Council (IWC). Other organizations can be found in Europe, such as the European Committee for Standardization (CEN) and the European Committee for Electrotechnical Standardization (CENELEC). In contrast, others are from Japan, such as the Japanese Industrial Standards Committee (JISC), or national bodies, such as the British Standards Institution (BSI). On the other hand, regulations are mandatory testing

procedures developed by governmental authorities such as the Economic Commission for Europe (UNECE), the National Highway Traffic Safety Administration (NHTSA) in the USA, or the Federal Motor Vehicle Safety Standards (FMVSS). These regulations have established a minimum level of safety performance for EVs, other vehicles, and vehicle equipment in order to guarantee safety needs [34,35].

The assessment process of standards and regulations consists of determining whether the tested device passes or fails the test based on the development of fire, explosion, rupture of components, or electrolyte leakage, among other factors [35]. A series of abuse tests that involve highly destructive scenarios have been developed in order to evaluate the battery's response under extreme circumstances, thereby ensuring the reliability of the devices, reducing the risk of TR, and certifying their safety [36]. The tests also indicate that the safety of the LIB needs to be guaranteed at each battery level: the battery cell, battery module, and battery pack. Therefore, each part must achieve the established requirements regarding mechanical, chemical, thermal, and electrical safety. Mechanical safety can be compromised when the device is subjected to sealing failure, collision, vibrations, or an impact [37]. The main tests employed to assess the safety regarding mechanical abuse are described in Table 1.

**Table 1.** LIB Mechanical abuse testing [36].

| Test | Description | Causes |
| --- | --- | --- |
| Nail penetration | Development of ISC. | The LIB is pierced with a nail that penetrates the separator in order to force an ISC. The ISC raises the heat inside the cell and causes SEI decomposition, which develops into exothermic side reactions that lead to TR. |
| Collision/Crush | Cells from the LIB are subjected to external load forces. The shell of the LIB breaks, causing the separator breakage. | When the cell interior receives the impact force, it experiences certain deformation, causing some cracks and internal displacement of the components. At higher compression, the separator can twist and stretch until it breaks and allows contact between both electrodes, which causes an ISC. To perform the test, the cell is placed on a flat surface and is crushed using a ribbed plate. The test is stopped when a certain level of deformation is reached, or when a voltage drop occurs. |
| Mechanical shock | Cells from the LIB are subjected to a multitude of shocks in both positive and negative directions at three mutually perpendicular orientations. | The cells receive shock forces due to the accelerations or decelerations of the EV. This test aims to test the robustness of the cell under sudden acceleration/deceleration. |
| Vibration | Cells from the LIB are subjected to long-term vibrations. | The vibration test aims to represent the vibrations that the LIB may experience during transport or driving in order to detect looseness of components such as electrical connectors. |

Although the following tests provide guidance regarding the LIB response under abusive conditions, they lack resemblance to real-life accidents. For instance, the LIB is placed at the bottom of the vehicle; therefore, it is susceptible to receiving an impact from any road element that could eventually damage it. However, to our knowledge, no existing test performs an assessment in that area. Therefore, there is a strong need for test revision and improvement, as current regulations employed in EVs and LIBs are based on internal combustion engine (ICE) vehicles, which are mainly based on front, rear, and side crashes. No specific test design for EVs has been developed. Accurate testing of the EV area surrounding the LIB would provide more knowledge regarding the welding points and the material breakage of the components that aim to protect the LIB. Therefore, the LIB position is worth analyzing during testing [38].

Another aspect that requires improvement in cell testing is the utilization of quasi-static tests to evaluate the cell response under mechanical loads, as they lack resemblance to an EV impact because the influence of velocity is not properly considered. The gaps

inside the battery pack make it difficult for the cells to perceive a quasi-static load, as they only start to receive the impact load when the pack is fully compressed [39], while in an actual EV crash, the cells receive a dynamic loading due to the kinetic energy of the impact.

The occurrence of a crush can lead to an ISC, which in turn can result in thermal abuse, as it is one of the primary sources of local heating. However, other events, such as mechanical shock, are less likely to develop into thermal or electrical abuse, as their influence on the LIB response is less severe compared to other abuse tests. Moreover, as has been mentioned in the previous section, the factors of degradation and SOC also have significant importance regarding the hazardous response of the LIB. For example, despite the fact that nail penetration could lead to fire propagation due to the occurrence of TR, the likelihood of this event occurring diminishes when the cells are charged at low SOC values [35].

## 3. Influential Factors on the LIB Response under Mechanical-Abuse Scenarios

LIB failure under mechanical abuse is a multi-physical process that involves mechanical failure, cell degradation, ISC, TR, and structure damage. Mechanical abuse refers to the effects of compression, impacts, and similar abuse conditions that could affect the LIB integrity [40]. Even though the presence of an ISC can visually indicate cell damage, internal damage does not always come to an imminent failure despite permanent changes have occurred. These effects in the cell components can be complicated to predict and to detect [41].

Therefore, two different concepts are going to be reviewed regarding cell state and cell damage. On the one hand, the presence of cracks and wrinkles on the separator after mechanical abuse that could lead to LIB failure. Then, considering that the degree of separator damage depends on the cell deformation caused by different compression effects [42], the results from a variety of compression tests are going to be reviewed. The separator porosity is an important factor that also needs to be considered when assessing the LIB behavior, as it has an influence on the ionic conductivity. A non-uniform porosity distribution affects the electric current and can result in lithium plating or dendrites [43]. Under mechanical loads, the separator can experience non-uniform stress and strain distributions, which change the porosity and thus the cell response [44].

On the other hand, it has been observed that the SOC level has a direct influence on the heat release after cell components breakage [45] because a higher SOC results in an earlier TR with a more severe exothermic reaction [46]. Finally, the effects of aging are also going to be reviewed, as the presence of degradation changes the LIB response under mechanical loading [47].

Taking into account the vehicle configuration, it can be observed that the side structure of the vehicle is stiffer than the front bumper. As a result, lateral impacts tend to be more severe than frontal crashes [48]. This indicates that the impact direction and the LIB arrangement on the EV also need to be examined, as LIB suffers from higher displacement under more severe impacts. Therefore, it is easier to cause an ISC [43]. The impact speed is also an external factor that could magnify the consequences of mechanical abuse due to its effects on LIB deformation and energy absorption [49].

This section will examine the influence of these effects on mechanical abuse regarding the development of an ISC and changes in the LIB performance by reviewing results from experimental data. The figures presented in this section have been recreated based on the data obtained from the literature review.

### *3.1. Compression's Influence on LIBs*

LIBs consist of the stacking and winding of multiple porous-material layers that suffer from deformation when subjected to mechanical loading. The force–displacement response of LIB changes depending on the loading conditions and cell structure that could cause shell compression [50]. Table 2 aims to summarize the most common compression tests for cylinder and prismatic cells [51].

**Table 2.** LIB compression testing [51].

| Test | Description | Cell Type |
|---|---|---|
| Bending | Upper cell layers experience compression while lower cell layers experience tension. | Cylinder cell<br>Prismatic cell |
| Penetration | Cause an ISC in a specific location through local deformation/fracture. | Cylinder cell<br>Prismatic cell |
| Indentation | Local deformation in the radial direction. | Cylinder cell |
| Out-plane/In-plane indentation | Reflects mechanical properties of LIB at in/out-plane directions. | Prismatic cell |
| Radial compression | Reflects mechanical properties in the radial direction. | Cylinder cell |
| Axial compression | Reflects axial properties of LIB. | Cylinder cell |
| In-plane/our-plane compression | Reflects mechanical properties at in/out-plane directions. | Prismatic cell |

The severity of the compression that a cell experiences from neighbouring cells due to mechanical loading and axial force changes its strain-rate dependency, separator properties, and electrode resistance due to the presence of buckling and enhanced stiffness that occur [28,35]. At the pack level, the structural integrity of the LIB can suffer from water ingress, deformation, and failure of the battery pack sealing due to road objects that penetrate the LIB [38].

When involved in an EV side impact or front impact, the LIB experiences different mechanical loadings. As described in Figure 2, a front crash causes in-plane loading, whereas a side crash causes out-of-plane impact loading [40,52].

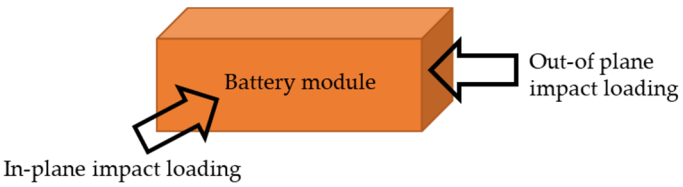


**Figure 2.** Impact loading directions.

The deformation stages of LIBs due to axial force have been evidenced in [53], where fully discharged 18650 cells were subjected to a quasi-static test, in which they were compressed at a loading speed of 5 mm/min. The main physical characteristics of the cells are described in Table 3.

**Table 3.** Physical characteristics of 18650 cells.

| Parameter | Value |
|---|---|
| Cell type | Cylinder |
| Height of the cell | 64.7 mm |
| Height of top end | 3.5 mm |
| Diameter of the cell | 18.2 mm |

The previous test indicates that the ISC occurs in the top region of the cell, where the jellyroll and shell casing are in contact. The bending of the shell casing punctuates the

separator, leading to the appearance of cracks and thinning, which cause the voltage drop because both electrodes get in contact. The test results indicate that the failure occurs at a compression of 4 mm, as a voltage drop due to ISC occurs at this stage. Figure 3 contains the representation of the results from the test in [53], which demonstrates that the voltage does not reach 0 V. Therefore, considering the complexity and risks of the residual voltage, specific LIB recycling protocols have been developed to address this issue [54].

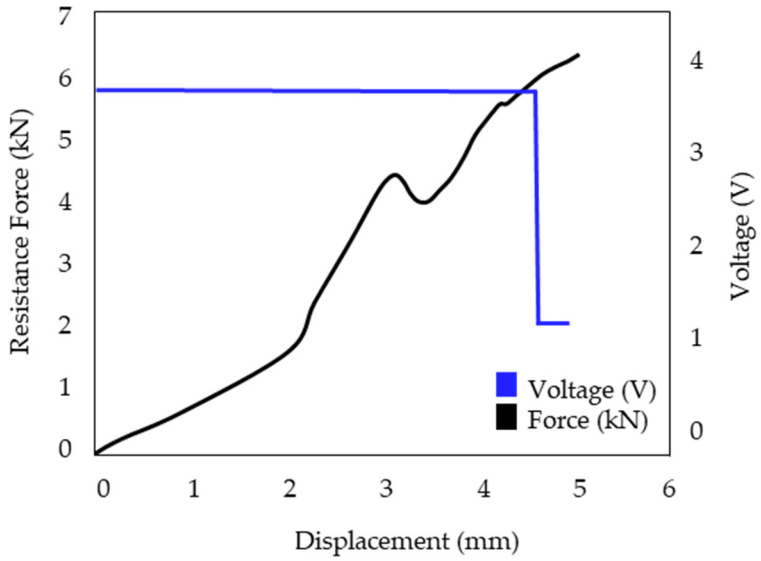


**Figure 3.** Representation of results of the axial compression test.

Figure 4, which is generated from [28], aims to describe the general tendency of cylinder 18650 cells deformation when compressed at 1 mm/min, 5 mm/min, and 10 mm/min. The physical aspects of the cells are described in Table 3. In the curve data, it can be observed that during initial loading, the displacement of the cell remains constant (stage 1) until it has been fully compressed and all remaining space within it has been consumed. Then, loading increases linearly until the maximum peak of force is reached (stage 2), which is followed by a sudden loading drop due to the breakage of internal components (stage 3). In general, higher loading entails higher displacement of the cell.

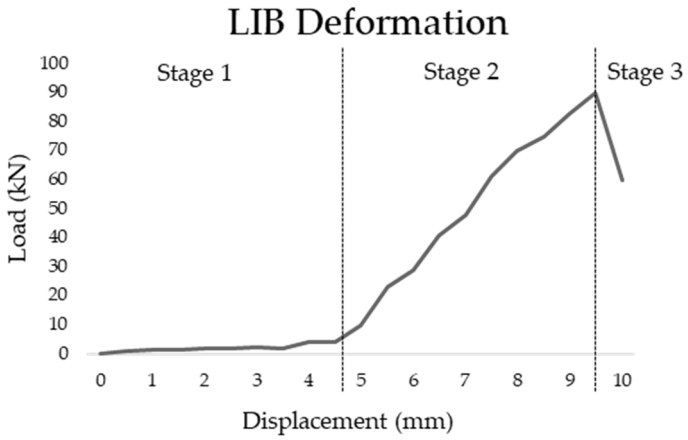


**Figure 4.** LIB deformation due to mechanical loading.

### *3.2. Influence of Impact Velocity and Battery SOC*

LIBs can be a resourceful component to power EVs because of their high energy density and long cycle life. However, a LIB malfunction could result in the release of toxic gases, fire, or even explosions, causing severe damage to vehicle occupants and nearby properties.

The literature indicates that there are two main factors that have an influence on the LIB response when exposed to mechanical loading that are difficult to control. These factors are the velocity and the SOC, which are arduous to regulate, as they may be contingent on the vehicle driver. The driving speed can have a significant influence on the LIB response, as the kinetic energy involved in case of collision is proportional to its value squared. Therefore, small increases in vehicle speed result in a significant increase in the impact severity [55,56].

The SOC level determines the energy contained inside the LIB. As a result, higher SOC implies higher electrochemical energy, which leads to intensive reactions with greater heat and gas release. Subsequently, cells with low SOC levels require greater damage in order to generate a TR [57].

The SOC influence on LIB failure when exposed to mechanical loads has been addressed in [58]. The testing process consisted of subjecting 18650 cells, which have the physical parameters described in Table 3, to compression and three-point bending tests as described in Figure 5. The compression test aims to assess the cells only in the radial direction, whereas the three-point bending test subjects upper cell layers to compression and lower layers to tension.

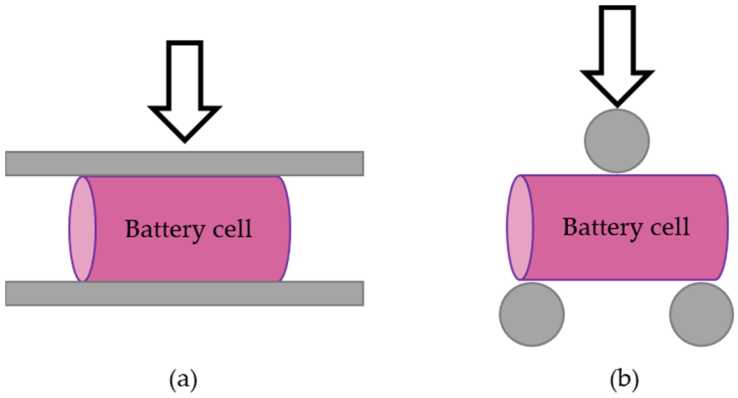


**Figure 5.** (**a**) Representation of compression test and (**b**) three-point bending test.

Both tests confirmed that a higher SOC increases cell stiffness due to the insertion of lithium ions in the anode and the deintercalation in the cathode. Even though the cathode stiffness is not affected by SOC changes, the results from the test confirm that the anode expands around 10% when increasing the SOC from 0 to 30%. Consequently, the overall compression increases by 20% for the above-mentioned SOC increase. The impact of the SOC on the voltage curve when the ISC occurs shows the following differences: on the one hand, the voltage at a low SOC drops immediately, whereas at a high SOC, the voltage drops progressively. This effect can be attributed to electron depletion, which is faster at low SOC. The results from the three-point bending test variant are represented in Figure 6 [58].

Cylinder 18650 LIBs were also subjected to uniaxial tension and three-point bending tests on [59] at 0.2 mm/min and 2 kN. The aim of this study was to determine the threshold limit for the rupture of the cell components. The analysis concluded that the stress generated on the cell due to tensile force should be between the yield stress limit (340 MPa) and the ultimate tensile strength (421 MPa), as over this value, the material failure is reached, and an ISC occurs to the LIB. The results from the axial compression demonstrate that stress is developed inside the cell due to the buckling of the components. The physical characteristics of the cells are also described in Table 3.

Further investigations of 18650 nickel cobalt aluminium oxide (NCA) cells were performed in [60], which tested different cell groups in order to obtain a correlation between the SOC and cell deformation caused by the interaction of surrounding cells. The physical parameters of the cell are described in Table 3, as both studies employed the same type of cells. These were loaded at a high SOC (SOC = 60% and V = 3.7 V) and low SOC

(SOC = 15% and V = 3.3 V). Moreover, this study also investigated the influence of the velocity by subjecting the cell to two different impact velocities (0.182 mm/s and 18.200 mm/s). The results from the test are represented in Figure 7, which shows that the stiffness of the LIB increases at higher SOC levels.

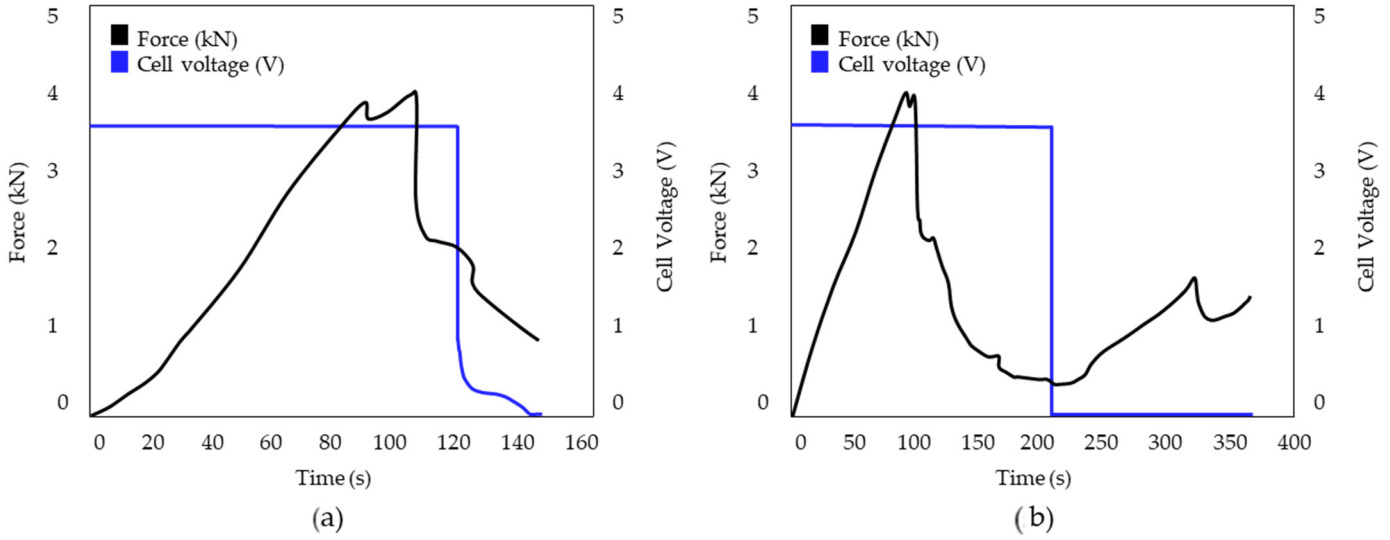


**Figure 6.** (**a**) Representation of the results from three-point bending tests with SOC at 10%. (**b**) Representation of the results from three-point bending tests with SOC at 70%.

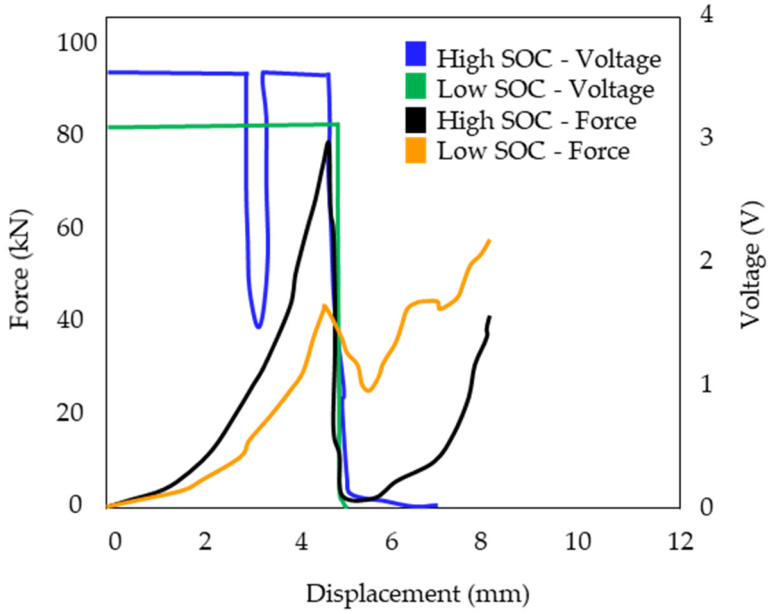


**Figure 7.** Effect of SOC at 0.182 mm/s.

Despite the curves from Figure 6 demonstrating that all tested cells ended with a voltage drop and the initiation of the ISC, the cells loaded at high SOC also experienced an early voltage drop that has been attributed to their stiffness decrease and the increase in electrode swelling. The early voltage drop can also be attributed to electrode contact due to the presence of dendrites. The voltage recovery can be attributed to the presence of leakage, which allowed the dendrites to move backward, reducing the pressure inside the LIB. Therefore, the SOC and deformation rate are strongly related to the LIB stiffness and electrode swelling, and thus cell failure. The energy accumulated in the LIB at higher SOC levels puts the performance of the LIB at risk, making it more susceptible to failure under mechanical loads. Therefore, at early displacements, it could experience voltage

drops without causing an ISC. These findings lead to the conclusion that working at low values of SOC increases the mechanical integrity of the cell [53,61]. The above-mentioned studies also remark on the difficulties of assessing mechanical failure before ISC, as fire and high temperatures damage the components, making it difficult to obtain feasible evidence of degradation. The results also recommend considering the velocity as a variable that has an influence on failure mechanisms.

The voltage recovery of the LIB described in Table 4 follows after an impact has been investigated in [61]. The high-acceleration impact was reproduced by means of a machete hammer that generates an impact pulse on the LIB, which is considered to be hazardous compared to an EV crash. The results of the voltage drop are represented in Figure 8. The voltage drop can be divided into three different stages: during the first one, the voltage experiences a slight drop, followed by a gradual rise, until it finally reaches a level slightly above the one from the previous stages.

**Table 4.** Physical characteristics of pouch cell from [61].

| Parameter | Value |
|---|---|
| Cell type | Polymer cell—Wuhan Kebia Battery Co. |
| Area of the cell | $16 \times 45$ mm$^2$ |
| Thickness of the cell | 4.8 mm |

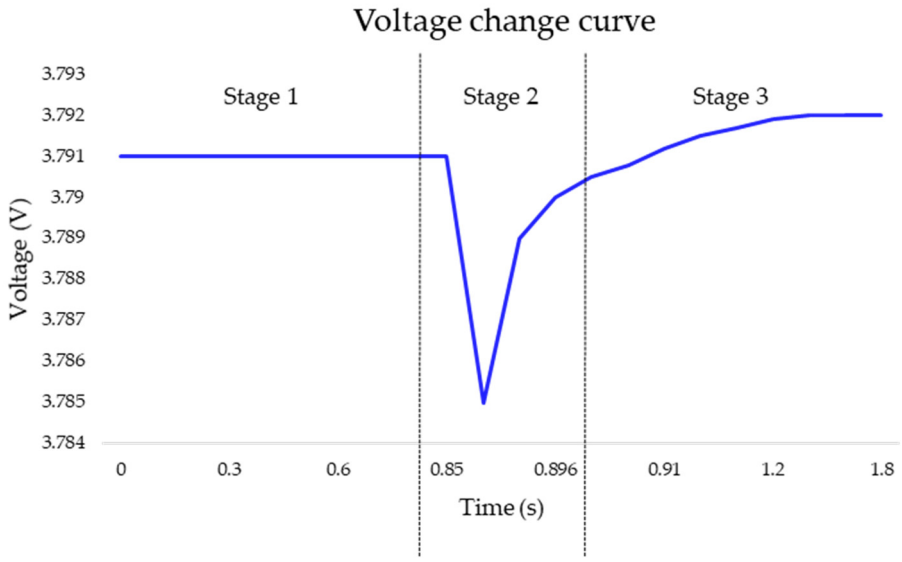


**Figure 8.** Voltage change due to machete hammer impact.

This study suggests that the relaxation effect of lithium ions in the dielectric caused by the impact force is the primary cause of the gradual rise in voltage following the impact. Therefore, increasing the impact acceleration also increases the voltage drop [61]. However, this voltage drop can also be caused by changes in the internal impedance that come from the decrease in the separator resistance during the impact, allowing the first contact between both electrodes. As previously mentioned in the assessment of previous tests, the induced pressure on the separator is one of the primary factors responsible for the voltage drop in conjunction with the ISC [60].

The influence of the SOC on pouch cells was also investigated in [62], wherein the authors performed a quasi-static test at an indentation velocity of 0.5 mm/min. The main physical features of the cell are described in Table 5. The analysis of the results shows that the influence severity of the SOC on pouch cells is much lower compared to cylinder cells. The results of the test are shown in Figure 9.

**Table 5.** Physical characteristics of cylinder cell from [62].

| Parameter | Value |
|---|---|
| Cell type | Pouch cell |
| Area of the cell | 150 × 242 mm$^2$ |
| Thickness of the cell | 7.2 mm |

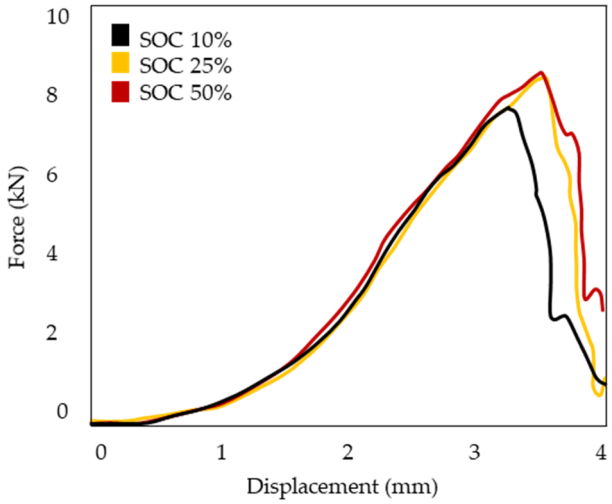


**Figure 9.** Representation of the indentation test results.

The obtained curve indicates that the voltage drop occurs at approximately 3.5 mm of intrusion, indicating the internal breakage of cell components and the emergence of an ISC. Changes in the curve tendency that occur around 2.5 mm of indentation have been attributed to the adhesion between the separator and anode layers, which increases with higher force levels. Continuous mechanical loading enhances the adhesion between the layers, eventually causing the molting of graphite particles from the anode and separator delamination. The presence of damage on cell layers eases the appearance of cracks and fractures that lead to the ISC.

In [63], the failure mechanisms of fully discharged pouch cells according to the characteristics of Table 6 were also evaluated. The test consisted of subjecting a series of pouch cells under compression force at 127 µm/s. The force–displacement curve obtained from the testing procedure is mainly affected by the porous materials of the cell (electrodes and separator). During the first stages of compression, the cell deformation depends on the densification of the electrodes. Then, the LIB displacement increases exponentially as the electrodes reach the maximum densification and cell layers are fully compacted. This study also tested pouch cells at 25 cm/s. The force–displacement curves of cells tested at different velocities are represented in Figure 10. The difference between the cell behavior under low speed and high speed can be attributed to the stiffening of the electrodes and the separator as the electrolyte fills the pores. The occurrence of the ISC also takes place earlier on cells tested at higher speed.

**Table 6.** Physical characteristics of pouch cell from [63].

| Parameter | Value |
|---|---|
| Cell type | Pouch cell |
| Area of the cell | 227 × 165 mm$^2$ |
| Thickness of the cell | 5.5 mm |

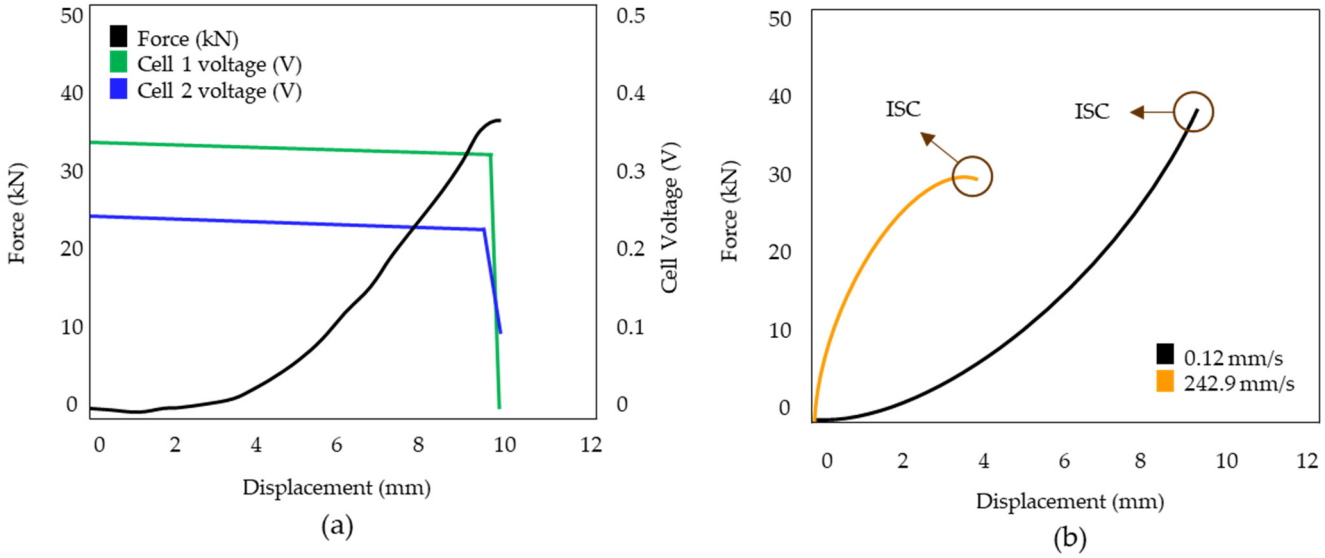


**Figure 10.** (**a**) Voltage drop due to cell failure and (**b**) Change in force–displacement as a function of deformation rate.

### *3.3. Influence of the Electrolyte and the Separator Thickness*

The influence of the electrolyte on the stiffness of the electrodes and separators is also emphasized in [64], where a drop test at low velocity was performed on the cell described in Table 7. The obtained findings suggest that at a distance of approximately 4 mm, the primary densification of the cell is attributed to a significant increment in deflection. Similar to the results from [61], a slight voltage drop followed by a voltage recovery occurs in the tested cells. The voltage drop has been associated with excessive separator thinning due to sheer stress, and the voltage rise comes from the recovery of elastic deformation from compressed layers. The initial voltage drop can evolve into an ISC if the impact energy is over 10 J. The electrodes can suffer from permanent damage due to the plastic deformation that causes the impact. The results from this study also indicate a capacity decrease and an internal resistance increase, as the tension and bending induced in cell components due to the impact causes a series of micro-cracks and the exfoliation of active materials, inducing a permanent loss of active material.

**Table 7.** Physical characteristics of pouch cell from [64].

| Parameter | Value |
|---|---|
| Cell type | Pouch cell |
| Area of the cell | 56 × 46 $mm^2$ |
| Thickness of the cell | 6 mm |

A dynamic test on elliptical and pouch cells that were initially discharged was performed in [65]. The physical characteristics of the tested cells are described in Table 8. The elliptical cell was tested at 5000 mm/s, and pouch cells were tested at 1 mm/s and 0.01 mm/s. The results from [65] demonstrate the voltage drop for cells tested at 1 mm/s occurs progressively; however, for cells tested at 0.01 mm/s, the voltage drops abruptly. However, it can be observed that the voltage drop occurs at the same displacement range (4 mm–5 mm) at each test.

**Table 8.** Physical characteristics of pouch cell.

| Parameter | Value |
|---|---|
| Cell type 1 | Elliptical cell |
| Area of the cell | 64 × 37 $mm^2$ |
| Thickness of the cell | 18 mm |
| Cell type 2 | Pouch cell |
| Area of the cell | 225 × 225 $mm^2$ |
| Thickness of the cell | 7.2 mm |

It can also be observed that the voltage of the pouch cells does not decrease to 0 V, meaning that they do not always come to an ISC when subjected to mechanical loading. The load, voltage, and displacement time histories of cell type 1 at different velocities are given in Figure 11, whereas the same results for cell type 2 are represented in Figure 12.

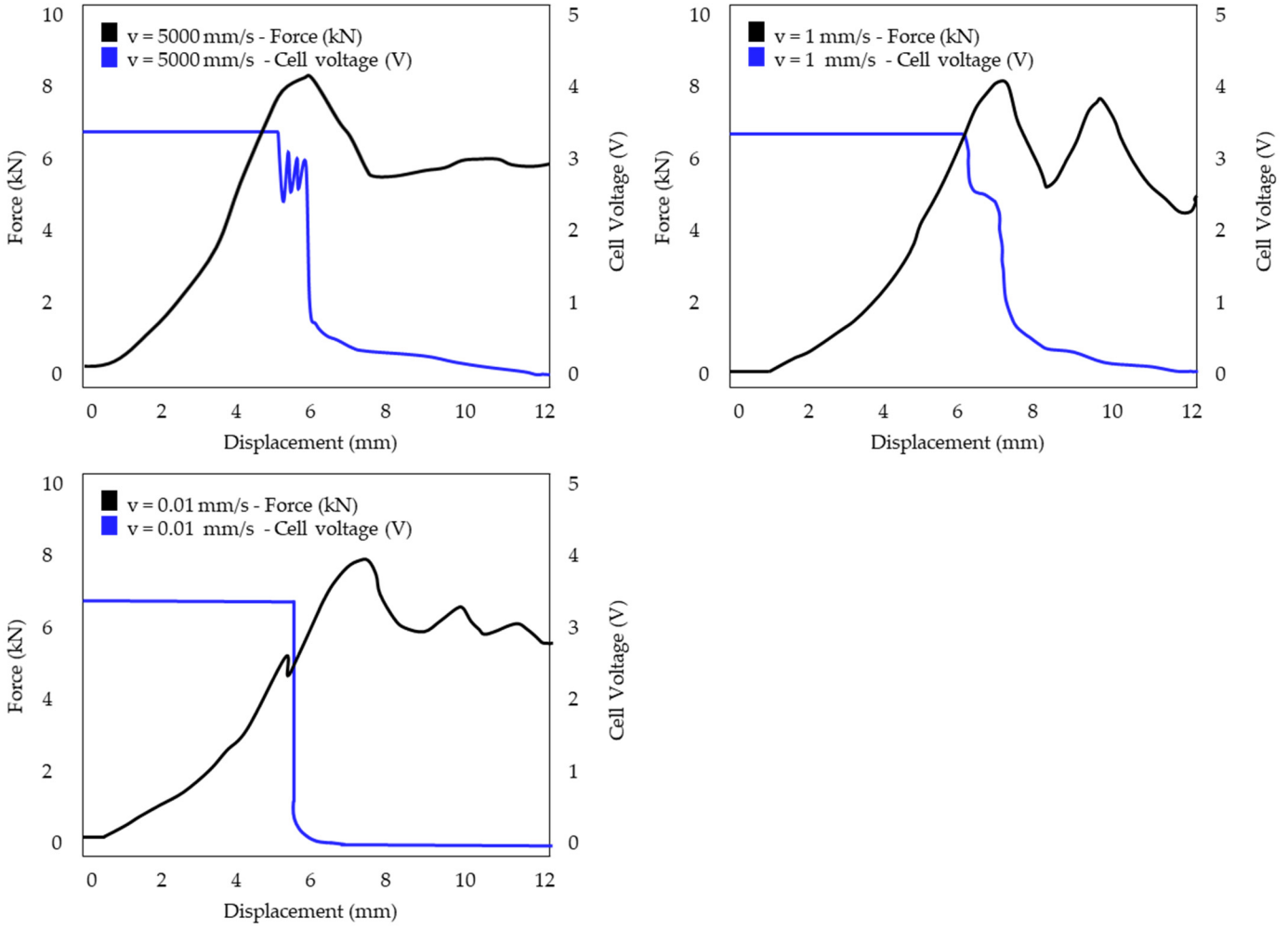


**Figure 11.** Load, voltage, and displacement time histories of elliptical cells tested at different velocities.

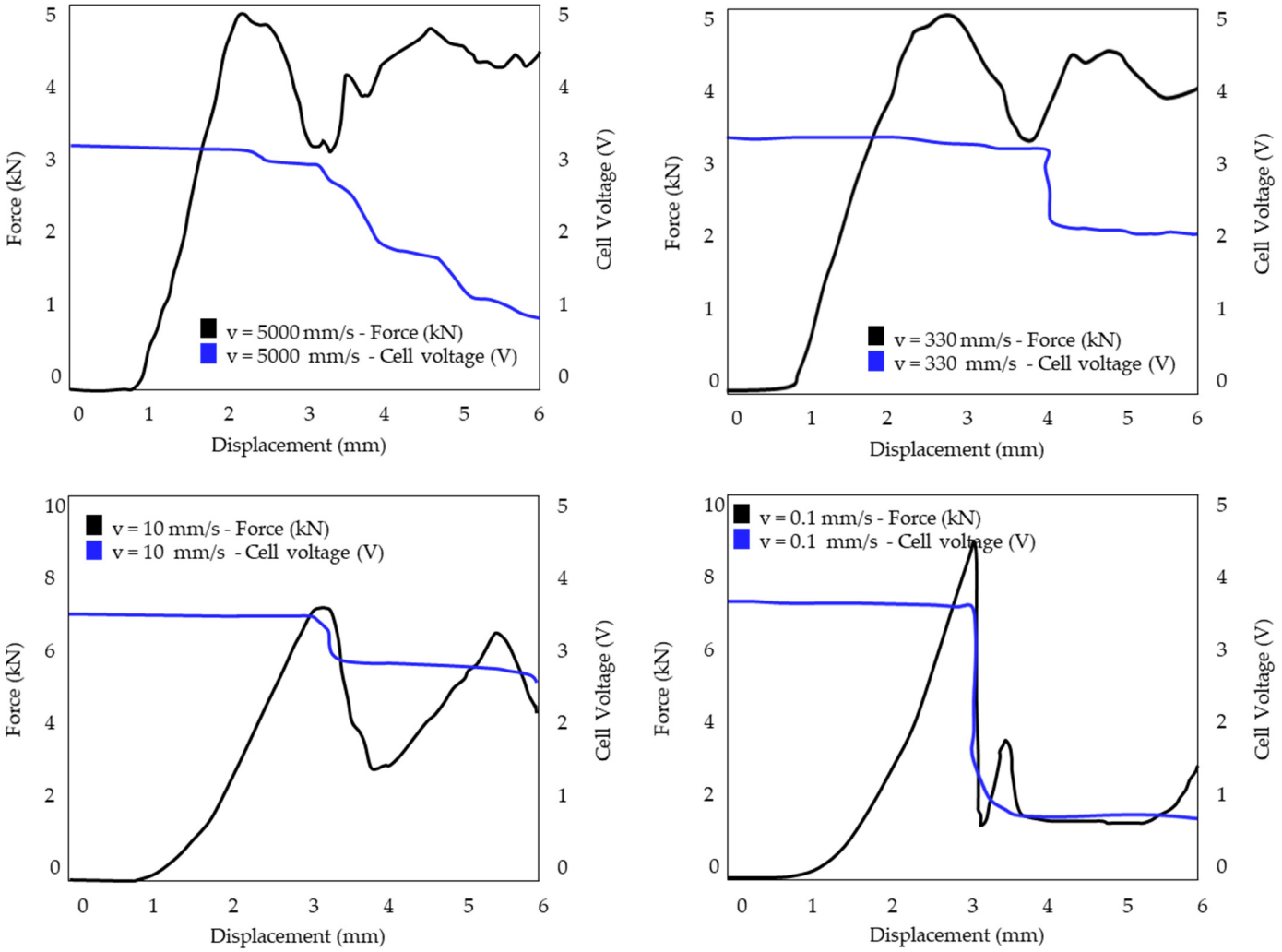


**Figure 12.** Load, voltage, and displacement time histories of pouch cells tested at different velocities.

### *3.4. Influence of Impact Direction*

The impact direction plays an important role regarding LIB safety, as the breakage of certain module areas could cause the whole casing to deform, causing a major number of cells to suffer from impact loading. For instance, impacts in the Z-direction, as described in Figure 13, can be more dangerous due to cell compaction and the lack of heat release that could evolve into a TR [31,66,67].

The influence of the impact direction has been investigated in [68]. The cells described in Table 9 were loaded at almost 0% SOC and subjected to quasi-static compression at 2 mm/min and a free-fall impact at 1 m/s and 5 m/s. The test was performed in X, Y, and Z directions, as described in Figure 13. The results from each test are represented in Figure 14. The results from the test at the X-direction demonstrate that different cell responses can be observed depending on the test speed. For instance, the jellyroll was barely deformed at a speed of 1 m/s; however, at a velocity of 5 m/s, the jellyroll experienced bulking and delamination. The force drop that can be observed in the curves occurs due to enclosure breakage, whereas force peaks are associated with jellyroll bulking and enclosure stretching.

Figure 14 also shows that as the load velocity decreases, the curve slope also decreases. The force rise can be attributed to the displacement increase, and force fluctuations can be attributed to the wrinkle of the enclosure and jellyroll. The folding of the jellyroll also entails a density increase, which causes the force to rise.

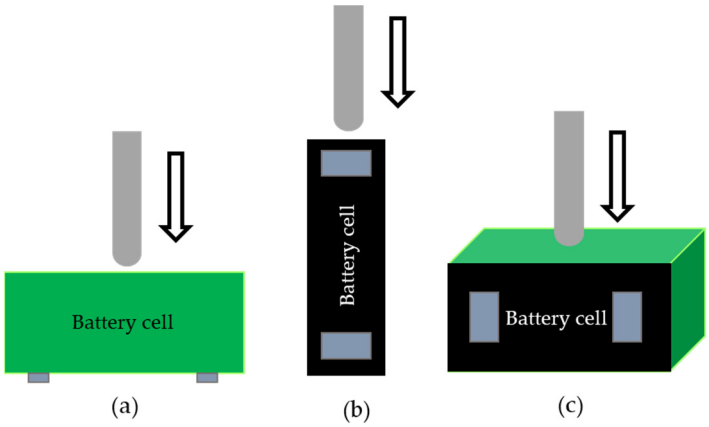


**Figure 13.** (**a**) Representation of X-direction impact; (**b**) Representation of Y-direction impact; (**c**) Representation of Z-direction impact.

**Table 9.** Physical characteristics of cylinder cell from [68].

| Parameter | Value |
|---|---|
| Cell type | Prismatic cell |
| Area of the cell | 220.0 × 102.5 $mm^2$ |
| Thickness of the cell | 66.5 mm |

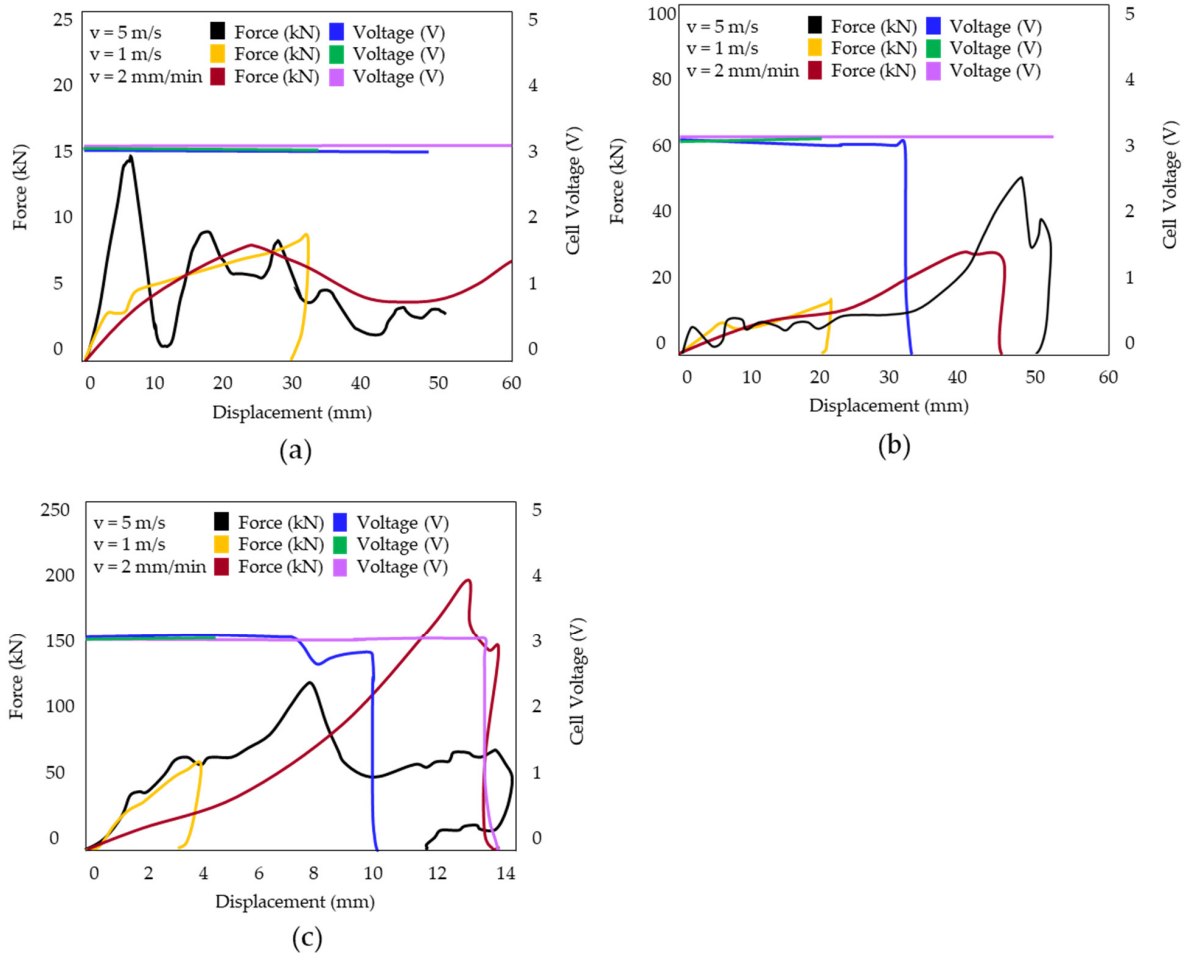


**Figure 14.** (**a**) Results representation of X-direction impact; (**b**) Results representation of Y-direction impact; (**c**) Results representation of Z-direction impact.

The results obtained in the Z-direction demonstrate that only the jellyroll that is close to the impactor is broken. The force drop has been associated with the jellyroll breakage, while the rebound at displacement recovery has been associated with the jellyroll rebound subsequent to the impact. The overall conclusion that can be drawn from the results is that prismatic LIB is more resilient to X-direction impacts due to the minimal presence of fluctuations. Nevertheless, the outcomes of the Z-direction test indicate that this is the most severe load case owing to the ISC that occurs at approximately 30 mm of displacement. The ISC is also present at the Z-direction due to the direct contact between both electrodes. However, before the ISC, a slight voltage drop occurs. The main failure mechanisms can be summarized as follows:

- X-direction: For cylinder impactors, the main failure mechanisms are fracture of the enclosure and bulking of the jellyroll. For the round impactor, the main failure source is the jellyroll fracture.
- Y-direction: Enclosure wrinkle, bulking, and delamination of the jellyroll.
- Z-direction: ISC occurs due to fracture of the jellyroll.

Subsequently, although the jellyroll delamination may not be the primary cause of the ISC, the fracture is. At a higher impact velocity, the elevated kinetic energy increases the probability of jellyroll rupture [68].

### *3.5. Influence of Aging*

It has been generally agreed that one of the major sources of LIB degradation is the aging process, as it is able to change their initial properties. The consequences of degradation aggravate when subjected to inappropriate temperature ranges, unbalanced SOC, or different stress factors that increase the degradation and failure mechanisms. The main contribution of degradation consists of the alteration of the steady state performance of LIB due to changes related to the interaction between the electrolyte and the electrodes, such as the solid electrolyte interphase (SEI) formation and lithium platting, which both involve a loss of lithium inventory (LLI) and loss of active material (LAM). Therefore, degradation can be associated with how much the electrode is available to host lithium and the quantity of lithium shifting between both electrodes, which can be detected through changes in variables such as voltage, state of health (SOH), SOC, or remaining useful life (RUL) [38,69].

The SOH is one of the main indicators of degradation, as it evaluates the health and performance of the LIB and provides information regarding battery aging and the current capacity of the cells. Another indicator of LIB aging is the decrease in capacity, which deteriorates the battery performance. This can be reflected through the SOC, which is the percentage of the maximum available capacity of the battery. The changes that can be observed on the voltage profile are primarily associated with the formation of SEI, as they originate from modifications on the open circuit potential (OCP) of electrodes [70,71].

The velocity of the degradation process also depends on other factors, such as the electrolyte chemistry, the battery design, the material composition, and the manufacturing process. In fact, the electrode chemistry can alter the electrode structure during the lithiation process, therefore developing different degradation patterns [70,72]. For instance, lithium ferrum phosphate (LFP) cells are more sensitive to degradation compared to nickel manganese cobalt (NMC). However, LFP cells have a more constant DC internal resistance (DCIR) and voltage degradation compared to NMC cells. An additional factor that contributes to cell degradation is the size of the LIB due to the fact that the degradation response of large-format cells differs from that of smaller cells, as they are subject to thermal inhomogeneity and a mechanical environment that causes an impact on the degradation tendency [73].

Even though there is very limited information currently available regarding the results of mechanical abuse on degraded cells, the influence of aging should be monitored in order to assess the performance of aged cells that are in service. Remarkable observations have been made regarding degradation and mechanical changes in aged LIB.

The main effect of aging on the LIB safety performance refers to the structural integrity of the electrodes, which could be triggered by inner cell stress due to charging/discharging [74]. This phenomenon plays an important role in capacity fading, as mechanical damage on the electrodes increases the LAM and causes rapid capacity fading [75,76].

However, aging seems to have positive effects regarding the thermal performance of LIBs. The authors of [77] observed that the lithium and electrolyte consumption to develop SEI reduces the quantity of active materials that participate in the exothermic reactions to develop TR. Furthermore, aged LIBs also release lower heat compared to pristine LIBs, which are able to maintain high temperatures for longer periods. Therefore, the presence of structural damage on the electrodes due to the aging process leads to a decrease in the TR onset temperature [78].

Regarding the effects of mechanical loading on aged cells, external compression increases the mechanical pressure inside the LIBs, reducing ionic transport, cell power, and capacity [79]. However, it has been observed that small deformations have a tendency to reverse aging effects when there is no ISC formation [80], as the generated pressure inside the cells increases the electrode density.

When aged LIBs are submitted to mechanical loading, their performance can differ from the performance of pristine LIBs. The authors of [81] observed an increase in failure deformation on aged cells that was attributed to the growth of the SEI layer from the anode and the stiffness reduction. The authors of [82] reached similar conclusions, as cells from their study also suffered from a right shift of the force–displacement curve. This effect could be attributed to the elastic behavior of the SEI layer, which allows the softening of the LIB in the early stages of compression [83].

The response of LIBs under mechanical loading was also investigated in [84], which compared the mechanical response of pristine and aged pouch cells with a nominal capacity of 41 Ah to quasi-static loading. The results from the test showed that new cells began venting after the formation of an ISC, which was followed by a severe internal temperature increase that led to TR. The results from aged cells were slightly different, as less venting could be observed before the TR. This event can be attributed to the capacity loss and LAM [85].

### *3.6. Discussion*

The results presented in this chapter demonstrate different LIB behaviors when subjected to mechanical loading. Although most of the results cannot be extrapolated and established as a general LIB behavior, a series of conjunction points that lead to similar results have been observed. Table 10 aims to summarize the results of tests performed on LIB.

Despite the fact that each study employed different testing protocols, the most remarkable finding is that in all instances, cell failure occurred when the displacement ranged between 3.3 mm and 5 mm, with the exception of the results obtained from [28], which were found to be approximately 9.5 mm. Nevertheless, this displacement increase can be attributed to the compression force, which is ten times greater than in other tests. Even though all LIBs suffered from a similar range of displacement, their shape and physical properties played a significant role in failure. For instance, the ISC of the cylinder cells from [53,60] occurs when the deformation reaches around 4.5 mm, which represents 7% and 28%, respectively, of the total cell height. However, although pouch cells from [62] fail when the indentation reaches around 3.5 mm, it represents 49% of the cell width. Hence, pouch cells will not undergo failure until half of the cell has been deformed, whereas smaller deformations are required in cylinder cells to cause mechanical and electrical failure.

During an impact, the velocity is another determinant parameter regarding failure, as there is a significant correlation between the loading rate and the velocity of the impact. Higher velocities entail higher stress, which results in an earlier and more severe failure of LIB. The fundamental mechanism of this phenomenon is believed to be the generated

kinetic energy, which causes different cell deformation [28,51], increasing the probability of fracturing the jellyroll and deteriorating the separator integrity [64,68].

**Table 10.** Results summary.

| References | Cell type | Test | Velocity | Max. Deflection |
|---|---|---|---|---|
| 53 | Cylinder | Quasi-static loading | 5 mm/min | 4.5 mm |
| 28 | Cylinder | Compression | 1 mm/min | 9.5 mm |
| 58 | Cylinder | 3-point bending and compression | 2 m/s–1.7 m/s | - |
| 60 | Cylinder | Surrounding cells | 0.182 mm/s–18.2 mm/s | 5 mm |
| 34 | Pouch–Polymer | High-speed flying ammunition | - | - |
| 62 | Pouch | Quasi-static loading | 0.5 mm/min | 3.3 mm–3.7 mm |
| 63 | Pouch | Compression | 25 cm/s | 10 mm |
| 64 | Pouch | Low velocity | 127 μm/s | 4 mm |
| 65 | Pouch and elliptical | Dynamic test | 0.01 mm/s–5000 mm/s | 4 mm–5 mm |
| 59 | Cylinder | Uniaxial tensions and 3 Point Bending | 0.2 mm/min | - |
| 52 | Cylinder | Quasi-static loading | 1 mm/min | - |

The velocity influence on LIBs can be assessed through dynamic and quasi-static loading tests. The process of failure due to quasi-static mechanical loads generally comprises a three-step progressive stiffness approach: in the early stages of compression, LIBs begin to compact while the empty spaces between internal components decrease. During the second stage of mechanical loading, the cell commences to perceive the mechanical load due to the interaction between its constituents. Subsequent deformation proceeds linearly until the LIBs experience a drastic increase in deformation, resulting in the initiation of the ISC, which can be observed through the reduction in the open circuit voltage (OCV) to 0 V and a temperature increase [39,86,87]. Dynamic tests are assumed to be more hazardous compared to quasi-static tests, as they involve higher kinetic energy and are more representative of a real EV impact since LIBs become stiffer and more vulnerable under these conditions. However, their set-up complexity limits the number of studies that perform this test [35,68].

When comparing both impact conditions, it can be observed that under quasi-static loading, all battery components are expected to fail at the same intrusion level due to sharp force; however, under dynamic loading, the collapse of the battery will consist of a more gradual process, as longer intrusion ranges are required to collapse. Subsequently, the ISC occurs at the force peak during the evaluation of quasi-static scenarios, whereas for dynamic tests, the voltage drop commences earlier than the occurrence of the ISC as cell components will have the combining deformation of tension and compression that will eventually lead to failure [88].

The occurrence of the ISC can be associated with the formation of internal cracks in the cell components and high stress levels in the loading direction [89,90]. In fact, failure mechanisms are different for tensile stress, compressive stress, or the combination of both due to their effects on the cell components' porosity [91,92]. The electrolyte has a significant

impact on the strain rate of LIB, as its interaction with the active material augments the compression resistance of various cell layers. For instance, the separator's porosity changes when immersed in the electrolyte, thereby affecting its compressibility and strain rate. The active materials derived from the electrodes are presented in a powdered form that is bonded together by the binder, resulting in a certain degree of porosity similar to porous foam materials. Then, cell deformation comes from compressing the pores between the active materials. Due to the porous structure of the electrodes, the presence of electrolytes can influence the cell response under impact loading; therefore, wet cells exhibit a higher strain-rate dependence, whereas dry cells exhibit a lower strain-rate dependence and thus have lower stiffness. This cell feature has the potential to be utilized in the crash safety assessment process, as polymeric wet separators are more likely to fail compared to dry separators [86,93,94].

LIB bending has significant effects on the separator integrity, as mechanical loading results in its maximum plastic strain, thereby favoring the emergence of cracks in its weakest regions, which in turn facilitates the contact between the anode and cathode, resulting in an ISC [95–97]. The presence of a slight voltage drop that occurs in different tests before reaching the ISC has been attributed to changes on the separator, as it suffers from thinning that causes a drop in the internal resistance of around 70%, instigating the appearance of non-uniform side reactions inside the cell. This slight voltage drop cannot be considered a failure mechanism, as mechanical loading can continue until the ISC occurs at higher forces. Separator thinning can be detected in force–displacement curves, as it originates changes in the curve slope [98].

The pressure that occurs inside the cell due to mechanical loads and the decrease in the separator resistance due to high acceleration impact can also lead to electrolyte leakage and energy loss, as the resistance of the impact is directly proportional to the thickness of the separator regardless of the impact stress. Then, thicker separators tend to reduce the voltage drop. Moreover, higher-thickness separators with greater-elasticity modules provide better resistance to impacts. In fact, the thickness of the separator has a direct impact on the discharge rate. This is due to the diffusion of ions, which require a larger distance to travel, resulting in slower ion transport. Therefore, the electrochemical reaction cannot be complete due to excess or lack of ions [88].

Voltage changes also depend on the SOC level, as at a low SOC, the voltage does not decrease at any point unless the deformation reaches the breakage limit and causes an ISC. However, higher SOC levels tend to inflate the LIB and increase the internal stress, which is also dependent on its shape. For example, the influence of the SOC on the mechanical integrity of cylinder and pouch cells is different [88]. The current working state and the heat generated by the high energy density of the LIB during the impact can also favor ISC development. Therefore, depending on the amount of energy stored in the LIB, a softer ISC may occur, resulting in a slight voltage drop and a slight temperature increase, whereas a more severe ISC may result from higher amounts of energy, causing a more significant and deeper voltage drop. Then, if the heat generated after the ISC is sufficient to increase the temperature of surrounding cells, it can trigger other ISCs that can lead to TR in the LIB. Nonetheless, the probability of the ISC to occur diminishes if there are no cracks observed in the separator [29,99]. In fact, most of the LIB tests performed in the laboratory have been fully discharged to reduce the energy dissipation and abrupt temperature.

Finally, further investigations should be performed regarding the influence of aging on the safety performance of LIBs when submitted to mechanical loading, as the LLI and LAM eventually decrease the amount of electrolyte, which causes an effect of cell drying and changes the LIB stiffness [100].

## 4. Conclusions

This review has assessed the influence of mechanical loading on the performance of LIBs through the analysis of the results obtained from subjecting several LIBs to impact forces capable of compromising their physical integrity, such as compression or three-point

bending tests. The primary conclusion that can be drawn from the previous data is that mechanical loading has direct effects on the LIB properties. The effects on the strain rate that lead to the hardening of the device, the fracture of its components, the rearrangement of cell layers, and the propagation of deformation throughout the entire LIB can result in permanent changes to its constituents, ultimately leading to failure. These impose additional requirements for LIB safety.

For instance, the origin of the ISC resulting from mechanical loading can be associated with component failure. Although it may not always result in TR, the persistent effects of impact from rough surfaces, road debris, or unexpected crushing may result in jellyroll fracture. Hence, the interaction between electrodes enhances the ISC effects and further induces thermal damage, ultimately leading to TR. The evaluated results provide plausible evidence that confirms this affirmation, as the presence of force drops comes from electrode and separator layers fracture, shell casing fracture, or a loss of stiffness.

The experimental evaluation of LIBs under mechanical loading also demonstrates that an influential factor regarding their outcome is the impact velocity. This phenomenon can be attributed to the differences in damage caused to different LIB areas. For impacts at higher speeds, the failure areas spread away from the point of impact, causing more damage to other areas [101,102]. Then, even though a single impact at high speed is sufficient to cause consistent damage to the LIB, continuous impacts at low speed are required to develop a hazardous situation. Therefore, the consequences of periodic soft impacts can eventually cause similar damage to one solid impact [102].

The effects of quasi-static impacts result in a more localized fracture area, causing smoother breakage. However, during dynamic testing, it is possible for the LIB structure to fracture completely, allowing the movement and detachment of the crushed area. Quasi-static intrusions also result in progressive stiffing, whereas dynamic impacts increase the damage propagation. Therefore, even a soft impact at high speed can induce enough damage to fracture the layered structure of the battery, allowing contact between both electrodes. The impact direction also has a significant influence on the structural integrity of the LIB, as under X-direction impact, the enclosure will fracture, and the jellyroll will bulk up, while under Y-direction impact, the enclosure will wrinkle, and the jellyroll will suffer from delamination and bulk up.

Another parameter that has a significant impact on mechanical failure is the dependence of the LIB strain on the SOC. Even though LIB failure mainly occurs due to changes in active materials, the results demonstrate that for cylinder cells, the stiffness tends to increase at higher SOC levels, as it is possible to observe a slight voltage decrease before reaching the ISC. However, despite the SOC influence on cylinder cells, no significant effects of this parameter can be detected regarding the mechanical integrity of pouch cells.

One of the main fundamental causes of LIB failure that can be identified from this review is the impact of mechanical loads on the separator integrity. The bending and local deformation of the separator due to compression leads to its thinning, followed by the formation of smaller fractures that entail a slight voltage drop before reaching a softer ISC. However, the breakage of a greater area of the separator leads to imminent failure as a larger area of contact between both electrodes occurs. A possible solution to address this issue would be to develop thicker separators in order to increase their elastic modulus and inhibit voltage reduction.

In addition, dry and wet separators have demonstrated different behaviors under mechanical loading due to the effects of the fluid interaction. Although these effects cannot be detected during low-speed impacts, they acquire greater significance during high-speed impacts. This is due to the hydrostatic pressure and viscosity of the electrolyte, which limits the force peak, Young's modulus, and the strength of the polymeric separator when soaked in electrolyte. Given that the peak force and the onset of ISC are triggered by separator failure, these factors explain why wet cells exhibit lower critical loads.

The attention given to the hazardous response of LIBs after mechanical loading has led to the need to develop improved standards and regulations to guarantee safe devices,

as the established regulation procedures lack resemblance to real-life scenarios and do not provide a thought assessment of the LIB.

On the one hand, the present standards and regulations entail a fundamental assessment of compliance with the testing requirements; however, they do not provide sufficient details regarding the internal modifications of the LIB despite not exhibiting any imminent failure indicators such as electrolyte leakage or an explosion. The outcome of various works leads to the conclusion that it is important to consider the constantly changing properties due to cycling in order to treat a brand new LIB and an overly charged and discharged LIB differently. The distinction between different chemistries and different cell shapes and LIB arrangements should also be taken into consideration, as their behavior may vary and should not be treated equally.

On the other hand, the resemblance between tests and realistic scenarios needs to be improved. For instance, the testing of vehicle components remains an unresolved issue owing to the inadequacy of their behavior when integrated into the entire EV, as the pressure from surrounding elements and interaction between the component and its protection systems may not be accurately represented. Furthermore, a majority of laboratory testing is based on quasi-static tests, although dynamic tests are a more accurate representation of reality.

Another drawback is that current standards and regulations are essentially based on conventional ICE vehicles and do not meet the requirements of EVs. For example, recent research suggests that battery pack installations may be exposed to vibration loads that are not considered in existing standards [34]. Hence, comprehensive data-gathering is required to scrutinize the primary deficiencies of EVs that warrant evaluation through testing and those that require revision.

**Author Contributions:** Conceptualization, M.C.-T., A.E.A. and H.V.-B.; methodology, M.C.-T., D.G.E., A.E.A. and H.V.-B.; validation, D.G.E., A.E.A. and H.V.-B., formal analysis, M.C.-T.; investigation, M.C.-T.; resources, A.E.A.; data curation, A.E.A. and H.V.-B.; writing—original draft preparation, M.C.-T.; writing—review and editing, A.E.A. and H.V.-B.; visualization, D.G.E., A.E.A. and H.V.-B.; supervision, A.E.A.; project administration, A.E.A.; funding acquisition, A.E.A. All authors have read and agreed to the published version of the manuscript.

**Funding:** This work was funded by MICIU/AEI/PID2020-120151RB-I00 and MICIU/AEI/PID2020-120151RB-I00/PID2019-111443RB-I00.

**Conflicts of Interest:** The authors declare no conflicts of interest.

## Abbreviation

| | |
|---|---|
| EV | Electric vehicle |
| LIB | Lithium-ion battery |
| ISC | Internal short circuit |
| TR | Thermal runaway |
| SOC | State of charge |
| SEI | Solid electrolyte interphase |
| LLI | Loss of lithium inventory |
| LAM | Loss of active material |
| SOH | State of health |
| RUL | Remaining useful life |
| OCP | Open circuit potential |
| LFP | Lithium Ferrum Phosphate |
| NMC | Nickel Manganese Cobalt |
| DCIR | DC internal resistance |
| ISO | International Organization for Standardization |
| SAE | Society of Automotive Engineers |
| IEEE | Institute for Electrical and Electronics Engineering |

| | |
|---|---|
| IWC | Infrastructure Working Council |
| CEN | European Committee for Standardization |
| CENELEC | European Committee for Electrotechnical Standardization |
| JISC | Japanese Industrial Standards Committee |
| BSI | British Standards Institution |
| UNECE | Economic Commission for Europe |
| NHTSA | National Highway Traffic Safety Administration |
| FMVSS | Federal Motor Vehicle Safety Standards |
| ICE | Internal combustion engine |
| NCA | Nickel cobalt aluminium oxide |
| OCV | Open circuit voltage |

## References


1. Sauer, D.U. Secondary Batteries: Lead-acid batteries–Lifetime Determing Processes. *Encycl. Electrochem. Power Sources* **2009**, 809–815. [CrossRef]
2. Zheng, S.; Wang, L.; Feng, X.; He, X. Probing the heat sources during thermal runaway process by thermal analysis of different battery chemistries. *J. Power Sources* **2018**, *378*, 527–536. [CrossRef]
3. Zhang, Z.J.; Ramadass, P.; Fang, W. Safety of lithium-ion batteries. In *Lithium-Ion Batteries*; Elsevier: Amsterdam, The Netherlands, 2014; pp. 409–435.
4. Zhao, C.; Sun, J.; Wang, Q. Thermal runaway hazards investigation on 18650 lithium-ion battery using extended volume accelerating rate calorimeter. *J. Energy Storage* **2020**, *28*, 101232. [CrossRef]
5. Chen, H.; Buston, J.E.H.; Gill, J.; Howard, D.; Williams, R.C.E.; Read, E.; Abaza, A.; Cooper, B.; Wen, J.X. A Simplified Mathematical Model for Heating-Induced Thermal Runaway of Lithium-Ion Batteries. *J. Electrochem. Soc.* **2021**, *168*, 010502. [CrossRef]
6. Liu, T.; Liu, Y.; Wang, X.; Kong, X.; Li, G. Cooling control of thermally-induced thermal runaway in 18,650 lithium ion battery with water mist. *Energy Convers. Manag.* **2019**, *199*, 111969. [CrossRef]
7. Sorensen, A.; Utgikar, V.; Belt, J. A Study of Thermal Runaway Mechanisms in Lithium-Ion Batteries and Predictive Numerical Modeling Techniques. *Batteries* **2024**, *10*, 116. [CrossRef]
8. Sun, T.; Wang, L.; Ren, D.; Shi, Z.; Chen, J.; Zheng, Y.; Feng, X.; Han, X.; Lu, L.; Wang, L.; et al. Thermal Runaway Characteristics and Modeling of LiFePO4 Power Battery for Electric Vehicles. *Automot. Innov.* **2023**, *6*, 414–424. [CrossRef]
9. Kvasha, A.; Gutiérrez, C.; Osa, U.; de Meatza, I.; Blazquez, J.A.; Macicior, H.; Urdampilleta, I. A comparative study of thermal runaway of commercial lithium ion cells. *Energy* **2018**, *159*, 547–557. [CrossRef]
10. Perea, A.; Paolella, A.; Dubé, J.; Champagne, D.; Mauger, A.; Zaghib, K. State of charge influence on thermal reactions and abuse tests in commercial lithium-ion cells. *J. Power Sources* **2018**, *399*, 392–397. [CrossRef]
11. Son, K.; Hwang, S.M.; Woo, S.-G.; Koo, J.K.; Paik, M.; Song, E.H.; Kim, Y.-J. Comparative study of thermal runaway and cell failure of lab-scale Li-ion batteries using accelerating rate calorimetry. *J. Ind. Eng. Chem.* **2020**, *83*, 247–251. [CrossRef]
12. Wu, T.; Chen, H.; Wang, Q.; Sun, J. Comparison analysis on the thermal runaway of lithium-ion battery under two heating modes. *J. Hazard. Mater.* **2018**, *344*, 733–741. [CrossRef]
13. Nerozzi, T.H.J.; Fox News. California Man's Tesla Catches Fire While Driving on Highway. 2023. Available online: https://www.foxnews.com/us/mans-tesla-catches-fire-while-driving-on-highway (accessed on 27 May 2024).
14. Abbott, K.C.; Buston, J.E.H.; Gill, J.; Goddard, S.L.; Howard, D.; Howard, G.E.; Read, E.; Williams, R.C.E. Experimental study of three commercially available 18650 lithium ion batteries using multiple abuse methods. *J. Energy Storage* **2023**, *65*, 107293. [CrossRef]
15. Huang, W.; Feng, X.; Han, X.; Zhang, W.; Jiang, F. Questions and Answers Relating to Lithium-Ion Battery Safety Issues. *Cell Rep. Phys. Sci.* **2021**, *2*, 100285. [CrossRef]
16. Feng, X.; Ouyang, M.; Liu, X.; Lu, L.; Xia, Y.; He, X. Thermal runaway mechanism of lithium ion battery for electric vehicles: A review. *Energy Storage Mater.* **2018**, *10*, 246–267. [CrossRef]
17. Wang, Q.; Mao, B.; Stoliarov, S.I.; Sun, J. A review of lithium ion battery failure mechanisms and fire prevention strategies. *Prog. Energy Combust. Sci.* **2019**, *73*, 95–131. [CrossRef]
18. Yu, Q.; Ma, L.; Yan, X. Modeling occupant injury severities for electric-vehicle-involved crashes using a vehicle-accident bi-layered correlative framework with matched-pair sampling. *Accid. Anal. Prev.* **2024**, *199*, 107499. [CrossRef] [PubMed]
19. Botton, I.N.; Takagi, D.; Shlez, A.; Yechiam, H.; Rosenbloom, E. Road accidents in children involving light electric vehicles cause more severe injuries than other similar vehicles. *Eur. J. Pediatr.* **2021**, *180*, 3255–3263. [CrossRef] [PubMed]
20. Zhu, J.; Zhang, X.; Luo, H.; Sahraei, E. Investigation of the deformation mechanisms of lithium-ion battery components using in-situ micro tests. *Appl. Energy* **2018**, *224*, 251–266. [CrossRef]
21. Lamb, J.; Orendorff, C.J. Evaluation of mechanical abuse techniques in lithium ion batteries. *J. Power Sources* **2014**, *247*, 189–196. [CrossRef]
22. Sheikh, M.; Elmarakbi, A.; Rehman, S. A combined experimental and simulation approach for short circuit prediction of 18650 lithium-ion battery under mechanical abuse conditions. *J. Energy Storage* **2020**, *32*, 101833. [CrossRef]

23. Cheng, Z.; Wang, C.; Mei, W.; Qin, P.; Li, J.; Wang, Q. Thermal runaway evolution of a 280 Ah lithium-ion battery with LiFePO4 as the cathode for different heat transfer modes constructed by mechanical abuse. *J. Energy Chemistry* **2024**, *93*, 32–45. [CrossRef]
24. Avdeev, I.; Gilaki, M. Structural analysis and experimental characterization of cylindrical lithium-ion battery cells subject to lateral impact. *J. Power Sources* **2014**, *271*, 382–391. [CrossRef]
25. Xu, J.; Liu, B.; Wang, X.; Hu, D. Computational model of 18650 lithium-ion battery with coupled strain rate and SOC dependencies. *Appl. Energy* **2016**, *172*, 180–189. [CrossRef]
26. Lin, C.; Burggräf, P.; Liu, L.; Adlon, T.; Mueller, K.; Beyer, M.; Wang, F. deep-dive analysis of the latest lithium-ion battery safety testing standards and regulations in Germany and China. *Renew. Sustain. Energy Rev.* **2023**, *173*, 113077. [CrossRef]
27. Lai, X.; Yao, J.; Jin, C.; Feng, X.; Wang, H.; Xu, C.; Zheng, Y. A review of lithium-ion battery failure hazards: Test standards, accident analysis, and safety suggestions. *Batteries* **2022**, *8*, 248. [CrossRef]
28. Xi, S.; Chang, L.; Chen, W.; Zhao, Q.; Guo, Y.; Cai, Z. Mechanical Response Analysis of Battery Modules Under Mechanical Load: Experimental Investigation and Simulation Analysis. *Energy Technol.* **2021**, *10*, 2100763. [CrossRef]
29. Chen, Y.; Kang, Y.; Zhao, Y.; Wang, L.; Liu, J.; Li, Y.; Li, B. A review of lithium-ion battery safety concerns: The issues, strategies, and testing standards. *J. Energy Chem.* **2021**, *59*, 83–99. [CrossRef]
30. Wang, W.; Yang, S.; Lin, C.; Shen, W.; Lu, G.; Li, Y.; Zhang, J. Investigation of mechanical property of cylindrical lithium-ion batteries under dynamic loadings. *J. Power Sources* **2020**, *451*, 227749. [CrossRef]
31. Xia, Y.; Chen, G.; Zhou, Q.; Shi, X.; Shi, F. Failure behaviours of 100% SOC lithium-ion battery modules under different impact loading conditions. *Eng. Fail. Anal.* **2017**, *82*, 149–160. [CrossRef]
32. Xiao, Y.; Yang, F.; Gao, Z.; Liu, M.; Wang, J.; Kou, Z.; Li, X. Review of mechanical abuse related thermal runaway models of lithium-ion batteries at different scales. *J. Energy Storage* **2023**, *64*, 107145. [CrossRef]
33. Li, H.; Zhou, D.; Zhang, M.; Liu, B.; Zhang, C. Multi-field interpretation of internal short circuit and thermal runaway behavior for lithium-ion batteries under mechanical abuse. *Energy* **2022**, *263*, 126027. [CrossRef]
34. Rehman, M.A.; Numan, M.; Tahir, H.; Rahman, U.; Khan, M.W.; Iftikhar, M.Z. A comprehensive overview of vehicle to everything (V2X) technology for Sustainable EV adoption. *J. Energy Storage* **2023**, *74*, 109304. [CrossRef]
35. Ruiz, V.; Pfrang, A.; Kriston, A.; Omar, N.; Van den Bossche, P.; Boon-Brett, L. A review of International Abuse Testing Standards and regulations for lithium ion batteries in electric and Hybrid Electric Vehicles. *Renew. Sustain. Energy Rev.* **2018**, *81*, 1427–1452. [CrossRef]
36. Lv, Y.; Geng, X.; Luo, W.; Chu, T.; Li, H.; Liu, D.; Li, C. Review on influence factors and Prevention Control Technologies of lithium-ion battery energy storage safety. *J. Energy Storage* **2023**, *72*, 108389. [CrossRef]
37. Yu, Q.; Nie, Y.; Peng, S.; Miao, Y.; Zhai, C.; Zhang, R.; Pecht, M. Evaluation of the safety standards system of power batteries for electric vehicles in China. *Appl. Energy* **2023**, *349*, 121674. [CrossRef]
38. Zhao, Z.; Liang, W.; Yang, X.; Cheng, H.; Ma, Y.; Ju, H.; Zhang, Y. An investigation on the ground impact of Electric Vehicle. *J. Phys. Conf. Ser.* **2022**, *2396*, 012030. [CrossRef]
39. Hu, L.; Zhang, Z.; Zhou, M.; Zhang, H. Crushing behaviors and failure of packed batteries. *Int. J. Impact Eng.* **2020**, *143*, 103618. [CrossRef]
40. Yiding, L.; Wenwei, W.; Cheng, L.; Xiaoguang, Y.; Fenghao, Z. Multi-physics safety model based on structure damage for lithium-ion battery under mechanical abuse. *J. Clean. Prod.* **2020**, *277*, 124094. [CrossRef]
41. Sahraei, E.; Campbell, J.; Wierzbicki, T. Modeling and short circuit detection of 18650 Li-ion cells under mechanical abuse conditions. *J. Power Sources* **2012**, *220*, 360–372. [CrossRef]
42. Greve, L.; Fehrenbach, C. Mechanical testing and macro-mechanical finite element simulation of the deformation, fracture, and short circuit initiation of cylindrical Lithium ion battery cells. *J. Power Sources* **2012**, *214*, 377–385. [CrossRef]
43. Luiso, S.; Fedkiw, P. Lithium-ion battery separators: Recent developments and state of art. *Curr. Opin. Electrochem.* **2020**, *20*, 99–107. [CrossRef]
44. Wang, Y.; Li, Q.; Xing, Y. Porosity variation of lithium-ion battery separators under uniaxial tension. *Int. J. Mech. Sci.* **2020**, *174*, 105496. [CrossRef]
45. Huang, P.; Yao, C.; Mao, B.; Wang, Q.; Sun, J.; Bai, Z. The critical characteristics and transition process of lithium-ion battery thermal runaway. *Energy* **2020**, *213*, 119082. [CrossRef]
46. Li, W.; Xia, Y.; Zhu, J.; Luo, H. State-of-Charge Dependence of Mechanical Response of Lithium-Ion Batteries: A Result of Internal Stress. *J. Electrochem. Soc.* **2018**, *165*, A1537–A1546. [CrossRef]
47. Ren, D.; Hsu, H.; Li, R.; Feng, X.; Guo, D.; Han, X.; Lu, L.; He, X.; Gao, S.; Hou, J.; et al. A comparative investigation of aging effects on thermal runaway behavior of lithium-ion batteries. *eTransportation* **2019**, *2*, 100034. [CrossRef]
48. Wang, G.; Wu, J.; Zheng, Z.; Niu, L.; Pan, L.; Wang, B. Effect of Deformation on Safety and Capacity of Li-Ion Batteries. *Batteries* **2022**, *8*, 235. [CrossRef]
49. Yiding, L.; Wenwei, W.; Cheng, L.; Xiaoguang, Y.; Fenghao, Z. A safety performance estimation model of lithium-ion batteries for electric vehicles under dynamic compression. *Energy* **2021**, *215*, 119050. [CrossRef]
50. Wang, G.; Guo, X.; Chen, J.; Han, P.; Su, Q.; Guo, M.; Song, H. Safety Performance and Failure Criteria of Lithium-Ion Batteries under Mechanical Abuse. *Energy* **2023**, *16*, 6346. [CrossRef]
51. Liu, B.; Jia, Y.; Yuan, C.; Wang, L.; Gao, X.; Yin, S.; Xu, J. Safety issues and mechanisms of lithium-ion battery cell upon mechanical abusive loading: A review. *Energy Storage Mater.* **2020**, *24*, 85–112. [CrossRef]

52. Zheng, G.; Tan, L.; Tian, G.; Yang, B.; Li, Q.; Sun, G. Dynamic crashing behaviors of prismatic lithium-ion battery cells. *Thin-Walled Struct.* **2023**, *192*, 110902. [CrossRef]
53. Zhu, J.; Zhang, X.; Sahraei, E.; Wierzbicki, T. Deformation and failure mechanisms of 18650 battery cells under axial compression. *J. Power Sources* **2016**, *336*, 332–340. [CrossRef]
54. Zanoletti, A.; Carena, E.; Ferrara, C.; Bontempi, E. A Review of Lithium-Ion Battery Recycling: Technologies, Sustainability, and Open Issues. *Batteries* **2024**, *10*, 38. [CrossRef]
55. Victor Chombo, P.; Laoonual, Y.; Wongwises, S. Lessons from the Electric Vehicle Crashworthiness Leading to Battery Fire. *Energies* **2021**, *14*, 4802. [CrossRef]
56. Khorasani-Zavareh, D.; Bigdeli, M.; Saadat, S.; Mohammadi, R. Kinetic energy management in road traffic injury prevention: A call for action. *J. Inj. Violence Res.* **2014**, *7*, 36–37. [CrossRef]
57. Doose, S.; Hahn, A.; Fischer, S.; Müller, J.; Haselrieder, W.; Kwade, A. Comparison of the consequences of state of charge and state of health on the thermal runaway behavior of lithium ion batteries. *J. Energy Storage* **2023**, *62*, 106837. [CrossRef]
58. Xu, J.; Liu, B.H.; Hu, D.Y. State of Charge Dependent Mechanical Integrity Behavior of 18650 Lithium-ion Batteries. *Sci. Rep.* **2016**, *6*, 21829. [CrossRef] [PubMed]
59. Manjunatha, M.; Manjunatha, R. Quasi-static failure analysis of lithium-ion battery (LIB) used in Electric Vehicle. *Mater. Today Proc.* **2023**, *90*, 169–174. [CrossRef]
60. Tsutsui, W.; Siegmund, T.; Parab, N.D.; Liao, H.; Nguyen, T.N.; Chen, W. State-of-charge and deformation-rate dependent mechanical behavior of electrochemical cells. *Exp. Mech.* **2017**, *58*, 627–632. [CrossRef]
61. Yu, D.; Ren, D.; Dai, K.; Zhang, H.; Zhang, J.; Yang, B.; You, Z. Failure mechanism and predictive model of lithium-ion batteries under extremely high transient impact. *J. Energy Storage* **2021**, *43*, 103191. [CrossRef]
62. Luo, H.; Xia, Y.; Zhou, Q. Mechanical damage in a lithium-ion pouch cell under indentation loads. *J. Power Sources* **2017**, *357*, 61–70. [CrossRef]
63. Kalnaus, S.; Wang, H.; Watkins, T.R.; Simunovic, S.; Sengupta, A. Features of mechanical behavior of EV battery modules under high deformation rate. *Extrem. Mech. Lett.* **2019**, *32*, 100550. [CrossRef]
64. Zhou, D.; Li, H.; Li, Z.; Zhang, C. Toward the performance evolution of lithium-ion battery upon impact loading. *Electrochim. Acta* **2022**, *432*, 141192. [CrossRef]
65. Kisters, T.; Sahraei, E.; Wierzbicki, T. Dynamic impact tests on lithium-ion cells. *Int. J. Impact Eng.* **2017**, *108*, 205–216. [CrossRef]
66. Essl, C.; Golubkov, A.; Thaler, A.; Fuchs, A. Comparing Different Thermal Runway Triggers for Automotive Lithium-Ion Batteries. *ECS Trans.* **2020**, *97*, 167–183. [CrossRef]
67. Raffler, M.; Sinz, W.; Erker, S.; Brunnsteiner, B.; Ellersdorfer, C. Influence of loading rate and out of plane direction dependence on deformation and electro-mechanical failure behavior of a lithium-ion pouch cell. *J. Energy Storage* **2022**, *56*, 105906. [CrossRef]
68. Zou, Z.; Xu, F.; Tian, H.; Niu, X. Testing and impact modelling of lithium-ion prismatic battery under quasi-static and dynamic mechanical abuse. *J. Energy Storage* **2023**, *68*, 107639. [CrossRef]
69. Taylor, J.; Barai, A.; Ashwin, T.R.; Guo, Y.; Amor-Segan, M.; Marco, J. An insight into the errors and uncertainty of the lithium-ion battery characterisation experiments. *J. Energy Storage* **2019**, *24*, 100761. [CrossRef]
70. Lin, C.; Xu, J.; Jiang, D.; Hou, J.; Liang, Y.; Zhang, X.; Mei, X. A comparative study of data-driven battery capacity estimation based on partial charging curves. *J. Energy Chem.* **2024**, *88*, 409–420. [CrossRef]
71. Chen, L.; Xie, S.; Lopes, A.M.; Li, H.; Bao, X.; Zhang, C.; Li, P. A new SOH estimation method for lithium-ion batteries based on model-data-fusion. *Energy* **2024**, *286*, 129597. [CrossRef]
72. Lee, J.; Sun, H.; Liu, Y.; Li, X. A machine learning framework for remaining useful lifetime prediction of Li-ion batteries using diverse neural networks. *Energy AI* **2024**, *15*, 100319. [CrossRef]
73. Gasper, P.; Saxon, A.; Shi, Y.; Endler, E.; Smith, K.; Thakkar, F.M. Degradation and modeling of large-format commercial lithium-ion cells as a function of chemistry, design, and aging conditions. *J. Energy Storage* **2023**, *73*, 109042. [CrossRef]
74. Müller, V.; Scurtu, R.; Memm, M.; Danzer, M.A.; Wohlfahrt-Mehrens, M. Study of the influence of mechanical pressure on the performance and aging of Lithium-ion battery cells. *J. Power Sources* **2019**, *440*, 227148. [CrossRef]
75. Li, Y.; Li, K.; Shen, W.; Huang, J.; Qu, X.; Zhang, Y.; Lin, Y. Stress-dependent capacity fade behavior and mechanism of lithium-ion batteries. *J. Energy Storage* **2024**, *86*, 111165. [CrossRef]
76. Friesen, A.; Horsthemke, F.; Mönnighoff, X.; Brunklaus, G.; Krafft, R.; Börner, M.; Risthaus, T.; Winter, M.; Schappacher, F.M. Impact of cycling at low temperatures on the safety behavior of 18650-type lithium ion cells: Combined study of mechanical and thermal abuse testing accompanied by post-mortem analysis. *J. Power Sources* **2016**, *334*, 1–11. [CrossRef]
77. Pastor, J.V.; García, A.; Monsalve-Serrano, J.; Golke, D. Analysis of the aging effects on the thermal runaway characteristics of Lithium-Ion cells through stepwise reactions. *Appl. Therm. Eng.* **2023**, *230*, 120685. [CrossRef]
78. Feinauer, M.; Abd-El-Latif, A.A.; Sichler, P.; Regalado, A.A.; Wohlfahrt-Mehrens, M.; Waldmann, T. Change of safety by main aging mechanism–A multi-sensor accelerating rate calorimetry study with commercial Li-ion pouch cells. *J. Power Sources* **2023**, *570*, 233046. [CrossRef]
79. Essl, C.; Golubkov, A.W.; Fuchs, A. Influence of Aging on the Failing Behavior of Automotive Lithium-Ion Batteries. *Batteries* **2021**, *7*, 23. [CrossRef]
80. Huang, P.; Liu, S.; Ma, J.; Zheng, G.; Li, E.; Wei, M.; Wang, Q.; Bai, Z. Comprehensive investigation on the durability and safety performances of lithium-ion batteries under slight mechanical deformation. *J. Energy Storage* **2023**, *66*, 107450. [CrossRef]

81. Sprenger, M.; Kovachev, G.; Dölle, N.; Schauwecker, F.; Sinz, W.; Ellersdorfer, C. Changes in the Mechanical Behavior of Electrically Aged Lithium-Ion Pouch Cells: In-Plane and Out-of-Plane Indentation Loads with Varying Testing Velocity and State of Charge. *Batteries* **2023**, *9*, 67. [CrossRef]
82. Liu, Y.; Xia, Y.; Xing, B.; Zhou, Q. Mechanical-electrical-thermal responses of lithium-ion pouch cells under dynamic loading: A comparative study between fresh cells and aged ones. *Int. J. Impact Eng.* **2022**, *166*, 104237. [CrossRef]
83. Shin, H.; Park, J.; Han, S.; Sastry, A.M.; Lu, W. Component-/structure-dependent elasticity of solid electrolyte interphase layer in Li-ion batteries: Experimental and computational studies. *J. Power Sources* **2015**, *277*, 169–179. [CrossRef]
84. Kovachev, G.; Ellersdorfer, C.; Gstrein, G.; Hanzu, I.; Wilkening, H.M.R.; Werling, T.; Schauwecker, F.; Sinz, W. Safety assessment of electrically cycled cells at high temperatures under mechanical crush loads. *eTransportation* **2020**, *6*, 100087. [CrossRef]
85. Birkl, C.R.; Roberts, M.R.; McTurk, E.; Bruce, P.G.; Howey, D.A. Degradation diagnostics for lithium ion cells. *J. Power Sources* **2017**, *341*, 373–386. [CrossRef]
86. Kotter, P.; Kisters, T.; Schleicher, A. Dynamic impact tests to characterize the crashworthiness of large-format lithium-ion cells. *J. Energy Storage* **2019**, *26*, 100948. [CrossRef]
87. Li, W.; Xia, Y.; Chen, G.; Sahraei, E. Comparative study of mechanical-electrical-thermal responses of pouch, cylindrical, and prismatic lithium-ion cells under mechanical abuse. *Sci. China Technol. Sci.* **2018**, *61*, 1472–1482. [CrossRef]
88. Pan, Z.; Li, W.; Xia, Y. Experiments and 3D detailed modelling for a pouch battery cell under impact loading. *J. Energy Storage* **2020**, *27*, 101016. [CrossRef]
89. Chung, S.H.; Tancogne-Dejean, T.; Zhu, J.; Luo, H.; Wierzbicki, T. Failure in lithium-ion batteries under transverse indentation loading. *J. Power Sources* **2018**, *389*, 148–159. [CrossRef]
90. Mo, F.; Tian, Y.; Zhao, S.; Xiao, Z.; Ma, Z. Working temperature effects on mechanical integrity of cylindrical lithium-ion batteries. *Eng. Fail. Anal.* **2022**, *137*, 106399. [CrossRef]
91. Sahraei, E.; Bosco, E.; Dixon, B.; Lai, B. Microscale failure mechanisms leading to internal short circuit in Li-ion batteries under complex loading scenarios. *J. Power Sources* **2016**, *319*, 56–65. [CrossRef]
92. Xing, B.; Xiao, F.; Korogi, Y.; Ishimaru, T.; Xia, Y. Direction-dependent mechanical-electrical-thermal responses of large-format prismatic Li-ion battery under mechanical abuse. *J. Energy Storage* **2021**, *43*, 103270. [CrossRef]
93. Kisters, T.; Gilaki, M.; Nau, S.; Sahraei, E. Modeling of dynamic mechanical response of Li-ion cells with homogenized electrolyte-solid interactions. *J. Energy Storage* **2022**, *49*, 104069. [CrossRef]
94. Dixon, B.; Mason, A.; Sahraei, E. Effects of electrolyte, loading rate and location of indentation on mechanical integrity of Li-ion pouch cells. *J. Power Sources* **2018**, *396*, 412–420. [CrossRef]
95. Zhang, C.; Xu, J.; Cao, L.; Wu, Z.; Santhanagopalan, S. Constitutive behavior and progressive mechanical failure of electrodes in lithium-ion batteries. *J. Power Sources* **2017**, *357*, 126–137. [CrossRef]
96. Huang, J.; Shen, W.; Lu, G. Mechanism of failure behaviour and analysis of 18650 lithium-ion battery under dynamic loadings. *Eng. Fail. Anal.* **2023**, *153*, 107588. [CrossRef]
97. Zhang, X.; Zhang, T.; Liu, N.; Yin, X.; Wu, X.; Han, H.; Wang, Q.; Zhang, Y. Dynamic crushing behaviors and failure of cylindrical lithium-ion batteries subjected to impact loading. *Eng. Fail. Anal.* **2023**, *154*, 107653. [CrossRef]
98. Zhang, X.; Sahraei, E.; Wang, K. Li-ion battery separators, mechanical integrity and failure mechanisms leading to soft and hard internal shorts. *Sci. Rep.* **2016**, *6*, 32578. [CrossRef]
99. Bulla, M.; Schmandt, C.; Kolling, S.; Kisters, T.; Sahraei, E. An experimental and numerical study on charged 21700 lithium-ion battery cells under dynamic and high mechanical loads. *Energies* **2022**, *16*, 211. [CrossRef]
100. Sevarin, A.; Fasching, M.; Raffler, M.; Ellersdorfer, C. Influence of cell selection and orientation within the traction battery on the crash safety of electric-powered two-wheelers. *Batteries* **2023**, *9*, 195. [CrossRef]
101. Xu, J.; Liu, B.; Wang, L.; Shang, S. Dynamic mechanical integrity of cylindrical lithium-ion battery cell upon crushing. *Eng. Fail. Anal.* **2015**, *53*, 97–110. [CrossRef]
102. Chen, X.; Yuan, Q.; Wang, T.; Ji, H.; Ji, Y.; Li, L.; Liu, Y. Experimental study on the dynamic behavior of prismatic lithium-ion battery upon repeated impact. *Eng. Fail. Anal.* **2020**, *115*, 104667. [CrossRef]